A Novel Empirical Potential for High-Temperature Molecular Dynamics Simulation of ThO_2 and MOX Nuclear Fuel Crystals

A. S. Boyarchenkov[1, a)], K. A. Nekrasov[1, 2, b)], A. Ya. Kupryazhkin[1] and Sanjeev K. Gupta[3]

[1]*Ural Federal University, 19 Mira St., Yekaterinburg, 620002, Russia*
[2]*Institute of High-Temperature Electrochemistry of the Ural Branch of the Russian Academy of Sciences, 20 Akademicheskaya St., 20, Yekaterinburg, 620990, Russia*
[3]*Computational Materials and Nanoscience Group, Department of Physics, St. Xavier's College, Ahmedabad 380009, India*

[a)]Corresponding author: boyarchenkov@gmail.com
[b)]kirillnkr@mail.ru

Abstract. Using a global optimization method, the parameters of a pair potential of the interaction of thorium and oxygen ions in ThO_2 are fitted, which are compatible with the potential set MOX-07 previously proposed for UO_2 and PuO_2 crystals. The potential is expressed in the form $U(R) = \exp(X – Y \cdot R)$ eV, and the optimal parameter values are $X = 8.073687$, $Y = 3.349$ Å^{-1}. Using these parameter values, the potential reproduces the lattice constant of the ThO_2 crystal in the entire temperature range up to melting, and quantitatively describes the high-temperature peak in the heat capacity that is associated with the superionic transition.

INTRODUCTION

Commercial nuclear reactors, burning mainly U-235, use only 1% of natural uranium. Even at the 2012 level of consumption, proven reserves of uranium in this regime will last 120 years only [1]. At the moment, there are two realistic alternatives to the classical uranium cycle that allow extending the life of nuclear energy for a long time. Firstly, these are fast neutron breeders with mixed U-Pu fuel. Secondly, these are thermal neutron breeders with mixed Th-U and Th-Pu fuel [2]. Thorium reserves exceed uranium by 3-4 times [3]; this can provide the world with energy for several thousand years [4].

The use of thorium fuel can also help solve such important problems of nuclear energy as the safety of nuclear power plants, the disposal of radioactive waste and non-proliferation. Thorium dioxide has a higher thermal conductivity and melting point than UO_2, which significantly reduces the risk of melting the reactor core. In addition, it has a low coefficient of thermal expansion and does not oxidize, which reduces the risks of a violation of the integrity of the fuel rod [5]. The production of minor actinides, which are the main contribution to the radiotoxicity of the irradiated fuel, is significantly reduced compared to the uranium and uranium-plutonium compositions, lowering the disposal costs [2]. Additionally, low plutonium production contributes to non-proliferation of nuclear materials. Protection against the proliferation is also provided by intense gamma radiation from the U-232 isotope, which makes it difficult to use the spent fuel for military purposes and is easily detected [6].

The experiments necessary for the study of thorium dioxide are expensive, since they require high temperatures (up to 3650 K), pressures, and radiation protection. Therefore, supplementing the experimental data with computer simulation is relevant. *Ab initio* modeling of actinide oxides is currently very limited by the size of the systems (96–324 ions) and the evolution time (picoseconds). Thus, molecular dynamics (MD) in the pair interaction

approximation remains in demand, as it can access systems of millions of particles [7] and evolution times of microseconds [8]. In this approximation, structural and transport properties of the system are determined by a set of pair potentials (SPP).

The parameterization of pair potentials can be based on *ab initio* calculations or empirical data. To the best of our knowledge, there are no first principle pair potentials for ThO_2 in the literature. Since 1985, a number of empirical potentials have been proposed, based on the lattice parameter, dielectric, elastic properties or dynamic calculation of temperature dependences, such as the thermal expansion and the bulk modulus change [9-15]. The global optimization of the potential parameters has rarely been discussed. The only known example of a global search for ThO_2 optimal parameter values [16] uses a stochastic genetic optimization algorithm based on the concepts of population, reproduction, mutation and generations from evolutionary biology.

In the present work, the empirical interaction potentials of the intrinsic ions in ThO_2 are fitted to complement the MOX-07 potential set [17] previously proposed for UO_2 and PuO_2. This potential set proved itself well in modeling the thermophysical properties, self-diffusion, melting, and crack propagation [7]. Common ionicity coefficients and O-O potential parameters now provide simulation of mixed oxides with an arbitrary content of U, Pu and Th.

POTENTIAL RECONSTRUCTION TECHNIQUE

In this work, thermal expansion data were selected as reference experimental data for the fitting of the potentials, since they are known with high enough accuracy [18]. To calculate the lattice constant at given temperatures, molecular dynamics NPT simulation was performed using the periodic boundary conditions (PBC). Newton's equations of motion were integrated by the Verlet method using the Berendsen thermostat and barostat. An original software package was applied that implements parallel computing on high-performance GPUs.

The global optimization of the parameters was carried out by the branching method with bisection and implicit estimation of the Lipschitz constant, which was proposed by S.I. Potashnikov in 2007 [19]. This method recursively splits the parameter search area into hyperintervals, choosing a point inside each of them, where the loss function is calculated. The bisection of a hyperinterval is performed so that: 1) there is a point with a calculated loss inside each of the two new hyperintervals; 2) the new point lies on a line between the old point and the farthest corner of the original hyperinterval; 3) the boundary between these two hyperintervals divides the distance between the points by the golden ratio $\varphi \approx 0.61803$. An illustration of such bisection is shown in Fig. 1.

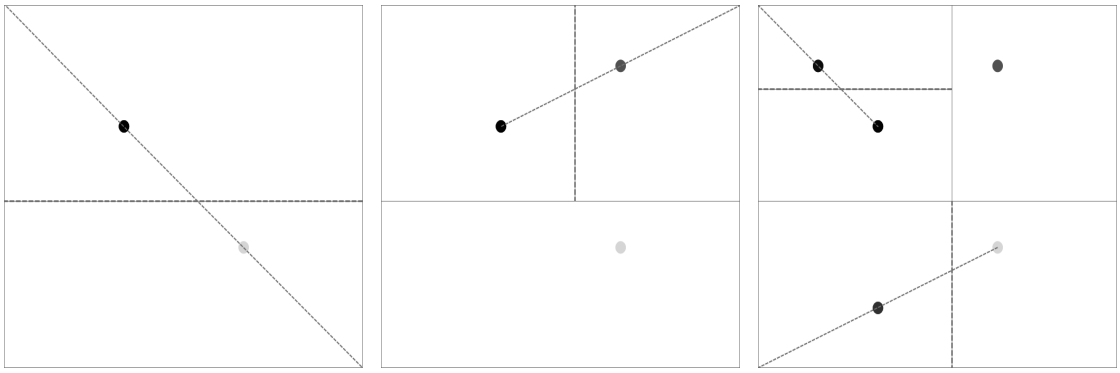

FIGURE 1. The first steps of the Potashnikov method. Left: the first bisection; the points lie on the diagonal connecting both corners. In the center: second bisection; a new point lies on the line connecting the first point and the angle. Right: bisection of two potentially optimal hyperintervals. Newly created boundaries of hyperintervals are shown by dashed lines. The darker color of the dots corresponds to the better values of the loss function.

The order of the bisection of hyperintervals was determined by the procedure of implicit estimation of the Lipschitz constant proposed in [20] for the DIRECT method. This procedure identifies a set of the promising hyperintervals by comparing their sizes and the corresponding magnitudes of the loss function, combining global and local search.

The potential of the valence interaction of thorium cations was assumed zero, since at the distances characteristic of the crystal it is small in comparison with the Coulomb repulsion. The potential Th-O was fitted in the Born-Mayer form

$$U(R) = \exp(X - Y \cdot R)\ \text{eV}, \quad (1)$$

where R is the distance between the ions.

Let us note that the Born-Mayer potential function is more often represented in the form $U(R) = A \cdot \exp(-Y \cdot R)$. Replacing the factor A with parameter X made it possible to increase the efficiency of the optimization method by limiting the range of the parameter to one order of magnitude.

An important advantage of the global optimization method is obtaining a map of the parameter space, instead of just one parameter set. This allows one to prove the existence of a unique solution to the problem, or to compare the differing solutions. Also, the map made it possible to see the exact solution, despite the presence of noise (statistical error) in the loss function. We divided the optimization problem into two, minimizing separately the deviation of the crystal lattice constant from the experiment at temperatures $T_1 = 500$ K and $T_2 = 2300$ K.

RESULTS AND DISCUSSION

The resulting solution maps are shown in Fig. 2. The thin black lines along the diagonal of the maps correspond to the solution of each of the subproblems.

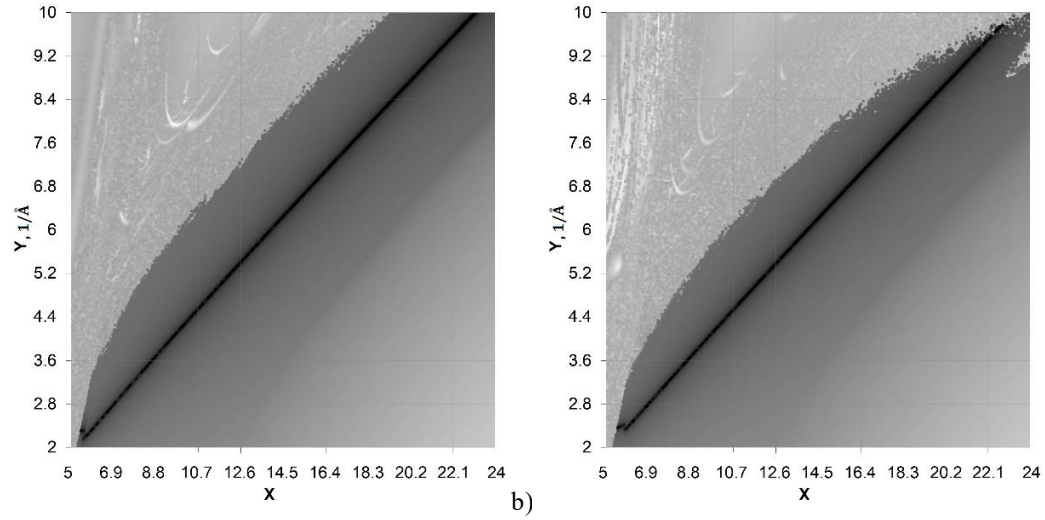

FIGURE 2. Maps for solving the problem of minimizing the deviation of the lattice constant at temperatures of 500 K (a) and 2300 K (b). The values of the minimized function correspond to points of different brightness, the darker the better.

One can see that for both temperatures, the whole considered region of parameter values is essentially divided into two parts: light and dark, and the boundary between them has a rather loose appearance. This sharp transition to the light tones corresponds to loss of the solid phase stability. In the lower left and upper right corners of the maps, the behavior of the system also becomes qualitatively different. At values of Y in the range 2.1–2.5 Å^{-1}, the melting temperature abruptly drops, the fluorite structure ceases to be stable (transitions to other phases occur), and thermal expansion in some cases becomes negative. On the other hand, at values of Y above 9 Å^{-1}, the melting temperature becomes too high, and the phase transition occurs without jumps in the density and energy of the system.

The optimal parameters (X, Y), which minimize the deviation of the lattice constant at both temperatures, lie at the intersection of the two black lines. However, we need two more steps to determine its position with sufficient precision. The slopes of these lines differs by less than 2%, but they are sensitive to the subset of points (choice of the range and the loss function threshold), which are used for approximation.

From data on Fig. 2, we determined that the intersection lies between $Y = 3.34$ Å^{-1} and $Y = 3.36$ Å^{-1}. Another global optimization was carried out in that region. The quadratic approximations of the obtained curves for $3.34 \le Y \le 3.36$ are as follows:

$$X(500\ \text{K}) = 0.0742754 \cdot Y^2 + 1.6373366 \cdot Y + 1.7571889, \quad (2)$$

$$X(2300\ \mathrm{K}) = 1.0828365 \cdot Y^2 - 5.0831567 \cdot Y + 12.952306. \quad (3)$$

The intersection of the curves (2) and (3) is at $Y \approx 3.349$ Å^{-1}. It is important to note, that such intersection of solutions of the subproblems gave more optimal set compared to the result of minimization of combined deviation of the lattice constant at both temperatures.

In order to illustrate this solution and its physical meaning, we run another series of simulations along the line (2) with Y in the range 3.3–3.4 Å^{-1}, estimating the corresponding deviation of the lattice constant. The dependence of this deviation at 2300 K on Y is shown in Fig. 3 (with the approximation line); while at 500 K the deviation was less than 0.0001 Å. This new approximation line intersects zero at $Y \approx 3.349$ Å^{-1} too. The corresponding value of X is calculated exactly according to (2). Thus, we propose the values of the parameters of the potential Th-O in the form (1) as $Y = 3.349$ Å^{-1} and $X = 8.073687$.

Representation of the parameter X with greater number of significant digits is necessary, since there is a possibility that decreasing the accuracy can unpredictably affect the behavior of the model. At the fixed value $Y = 3.349$ Å^{-1}, the derivatives of the lattice constant L with respect to X in the vicinity of the optimal value were $dL(500\ \mathrm{K})/dX \approx 0.98$ Å and $dL(2300\ \mathrm{K})/dX \approx 0.99$ Å. This means, for example, that an increase in X by 0.001 would lead to an increase in L by 0.001 Å. This error exceeds the difference between the calculated and experimental values of the lattice constant in the whole temperature range from 0 K to 2500 K (Fig. 3).

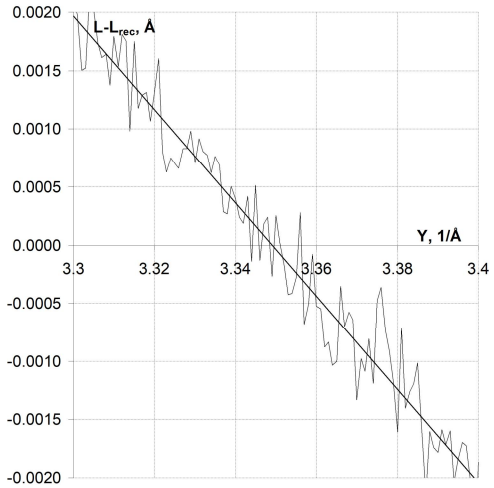

FIGURE 3. Deviation of the lattice constant from the recommendation [18] at 2300K calculated using series of Th-O potentials along the line (2).

As the modeling in this work has shown, the optimal parameters allow reproducing the ThO_2 lattice constant and the heat capacity in the temperature range from 500 K up to melting. The lattice constant at 500 K and 2300 K is reproduced perfectly, which proves the high quality of the chosen global optimization methodology. The notable deviation of the thermal expansion from the recommendation [18] is observed only at temperatures of 2700 K and higher (Fig. 4), since this recommendation is based on experiments at temperatures up to 2400 K, and therefore does not take into account the existence of a second-order superionic phase transition near 3000 K. However, this transition manifests itself in the form of a heat capacity peak, which in our model corresponds to experimental data [21] (Fig. 5).

On Fig. 5, one can see different views on the behavior of the heat capacity in the superionic transition region. The recommendation of Fink [22] assumes the abrupt change of the heat capacity near 3000 K. The experimental data of Ronchi and Hiernaut [21] shows almost smooth peak, which seems very similar to our model results. Our simulations of UO_2 also support the smooth transition with gradual change of the heat capacity magnitude [17], the thermal expansion coefficient and the activation energy of anion self-diffusion [24]. Finally, the recent recommendation of Konings et al. [23] assumes monotonic growth of the heat capacity with temperature. Such behavior has not been supported by experimental data yet.

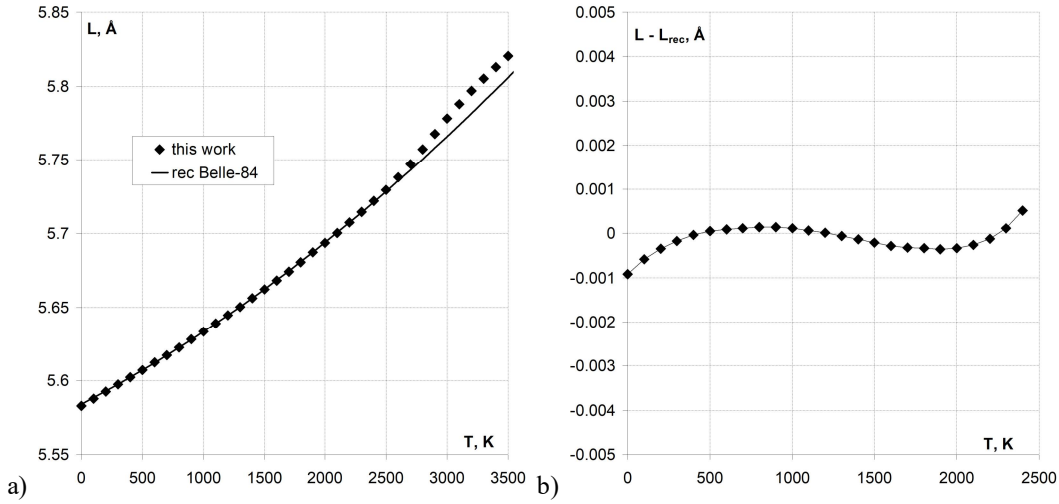

FIGURE 4. The calculated temperature dependences of the lattice constant (a) and its deviation from the experimental recommendation (b).

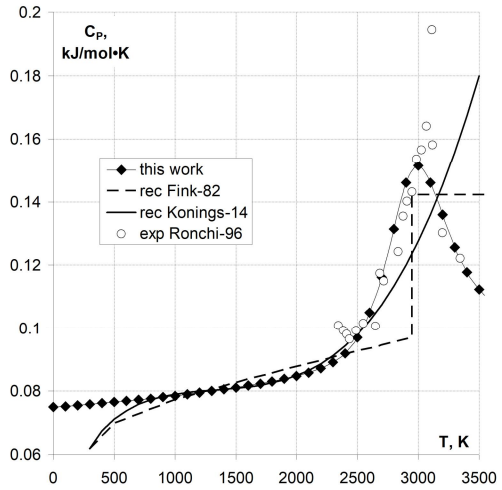

FIGURE 5. Temperature dependence of the isobaric heat capacity in comparison with experimental data: Ronchi-96 [21], Fink-82 [22], Konings-14 [23].

CONCLUSION

The task of reconstructing the empirical potentials of interaction between the intrinsic ions of thorium dioxide is for the first time solved by the approach of complete global optimization of parameters. The problem is divided into two subtasks, with the idea of finding the optimal parameters as the intersection of the solutions of these subtasks. Solutions to the subtasks (at temperatures of 500 K and 2300 K) on the maps of two-parameter space are obtained in the form of continuous lines. The optimal parameters obtained at the intersection of these lines ensured the exact reproduction of thermal expansion, the heat capacity, and the heat capacityλ-peak corresponding to the superionic transition. In the future, the implemented methodology will allow a detailed analysis of the influence of potential parameters on thermophysical and elastic properties, showing the full potential of the approximation of rigid ions and pair potentials. The proposed method can also be applied to solve the more complex multi-dimensional problem of reconstructing a new set of empirical pair potentials for actinide oxides, improving the current MOX-07 approximation.

ACKNOWLEDGMENTS

The study was funded by the Russian Foundation for Basic Research (RFBR) according to the research project No. 16-52-48008.S.K. Gupta thanks the Department of Science and Technology (India) and the Russian Foundation for Basic Research (Russia) for the financial support (Grant no.: INT/RUS/RFBR/IDIR/P-6/2016).

REFERENCES

1. "Uranium 2014: Resources, Production and Demand," A Joint Report by the OECD Nuclear Energy Agency and IAEA, 2014. URL: https://www.oecd-nea.org/ndd/pubs/2014/7209-uranium-2014.pdf (accessed: 13.07.2020).
2. S. David, E. Huffer, H. Nifenecker, Europhysics News **38(2)**, 24–27 (2007).
3. "World Thorium Occurences, Deposits and Resources," IAEA-TECDOC-1877, International Atomic Energy Agency, Vienna, 2019. URL: http://www-pub.iaea.org/MTCD/Publications/PDF/TE-1877web.pdf (accessed: 13.07.2020).
4. P. Martin, D. J. Cooke, R. Cywinski, Journal of Applied Physics **112**, 073507 (2012).
5. B. Szpunar, J. Szpunar, Physics International **4(2)**, 110–119 (2013).
6. "Thorium fuel cycle – Potential benefits and challenges," IAEA-TECDOC-1450, International Atomic Energy Agency, Vienna, 2005. URL: http://www-pub.iaea.org/MTCD/Publications/PDF/TE_1450_web.pdf (accessed: 13.07.2020).
7. H. Balboa, L. Van Brutzel, A. Chartier, Y. Le Bouar, Journal of Nuclear Materials **495**, 67–77 (2017).
8. A. S. Boyarchenkov, S. I. Potashnikov, K. A. Nekrasov, A. Ya. Kupryazhkin, Journal of Nuclear Materials **442**, 148–161 (2013).
9. G. V. Lewis, C. R. A. Catlow, J. Phys. C: Solid State Phys. **18**, 1149–1161 (1985).
10. R. K. Behera, C. S. Deo, J. Phys.: Condens. Matter **24**, 215405 (2012).
11. M. Osaka, J. Adachi, K. Kurosaki *et al.*, Journal of Nuclear Science and Technology **44(12)**, 1543–1549 (2007).
12. T. Arima, K. Yoshida, T. Matsumoto *et al.*, Journal of Nuclear Materials **445**, 175–180 (2014).
13. M. W. D. Cooper, M. J. D. Rushton, R. W. Grimes, J. Phys.: Condens. Matter **26**, 105401 (2014).
14. J.-J. Ma, J.-G. Du, M.-J. Wan, G. Jiang, Journal of Alloys and Compounds **627**, 476–482 (2015).
15. H. Xiao, C. Long, X. Tian, H. Chen, Materials and Design **96**, 335–340 (2016).
16. P. S. Ghosh, Y. S. Ranawat, A. Arya, G. K. Dey, AIP Conference Proceedings **1665**, 140035 (2015).
17. S.I. Potashnikov, A.S. Boyarchenkov, K.A. Nekrasov, A.Ya. Kupryazhkin, Journal of Nuclear Materials**419**, 217–225 (2011).
18. J. Belle, R.M.Berman "Thorium dioxide: properties and nuclear applications," Naval Reactors Office, U.S. Dep. Of Energy, 1984. URL: https://inis.iaea.org/collection/NCLCollectionStore/_Public/16/071/16071971.pdf (accessed: 13.07.2020)
19. S. I. Potashnikov (private communication).
20. D. R. Jones, C. D. Perttunen, B. E. Stuckman, Journal of optimization theory and application **79(1)**, 157–181 (1993).
21. C. Ronchi, J. P. Hiernaut, Journal of Alloys and Compounds **240**, 179–185 (1996).
22. J. K. Fink, Int. J. Thermophys. **3(2)**, 165–200 (1982).
23. R. J. M. Konings, O. Benes, A. Kovacs *et al.*, Journal of Physical and Chemical Reference Data **43**, 013101 (2014).
24. S. I. Potashnikov, A. S. Boyarchenkov, K. A. Nekrasov, A. Ya. Kupryazhkin, Journal of Nuclear Materials **433**, 215–226 (2013).
25. A. S. Boyarchenkov, S. I. Potashnikov, K. A. Nekrasov, A. Ya. Kupryazhkin, Journal of Nuclear Materials **427**, 311–322 (2012).